Endocrine (2016) 52:380–390
DOI 10.1007/s12020-015-0747-y

ORIGINAL ARTICLE

Lithium prevents rat steroid-related osteonecrosis of the femoral head by β-catenin activation

Zefeng Yu[1] · Lihong Fan[1] · Jia Li[1] · Zhaogang Ge[1] · Xiaoqian Dang[1] · Kunzheng Wang[1]

Received: 5 June 2015 / Accepted: 18 September 2015 / Published online: 12 October 2015

Abstract This study explored the use of lithium to prevent rat steroid-related osteonecrosis of the femoral head (ONFH) through the modulation of the β-catenin pathway. ONFH was induced by methylprednisolone combined with lipopolysaccharide, and serum lipids were analyzed. ONFH was detected by hematoxylin–eosin staining. Micro-CT-based angiography and bone scanning were performed to analyze vessels and bone structure, respectively. Immunohistochemical staining for peroxisome proliferator-activated receptor gamma (PPARγ), bone morphogenetic protein-2 (BMP-2), and vascular endothelial growth factor (VEGF) was analyzed. Protein levels of phospho-glycogen synthase kinase-3β at Tyr-216 (p-Tyr^{216} GSK-3β), total glycogen synthase kinase-3β (GSK-3β) and β-catenin, as well as mRNA levels of GSK-3β and β-catenin in femoral heads, were assessed. The rate of empty bone lacunae in the femoral heads was lower in the lithium and control groups than in the model group. The lithium group showed preventive effects against steroid-related vessel loss by micro-CT-based angiography and VEGF staining. Lithium treatment improved hyperlipidemia and reduced PPARγ expression. Moreover, lithium improved steroid-related bone loss in micro-CT bone scans and BMP-2 staining analyses. Furthermore, local β-catenin was reduced in steroid-related ONFH, and lithium treatment increased β-catenin expression while reducing p-Tyr^{216} GSK-3β levels. The local β-catenin pathway was inhibited during steroid-related ONFH. Lithium may enhance angiogenesis and stabilize osteogenic/adipogenic homeostasis during steroid-related ONFH in rats by activating the β-catenin pathway.

Keywords Lithium · Steroid-related osteonecrosis · β-Catenin pathway · Angiogenesis · Osteogenic/adipogenic differentiation disturbance

Introduction

Recently, steroid-related osteonecrosis of the femoral head (ONFH) has widely occurred in patients with autoimmune diseases after high-dose corticosteroid treatment [1, 2]. There are a variety of treatment methods for this disease, such as reducing weight bearing activity, drug therapy, core decompression, and artificial joint replacement [3]. However, the ideal treatment remains unclear because all of these methods simply focus on preventing irreversible complications. Although the etiology of steroid-related ONFH has not been fully elucidated, perturbation of osteogenic/adipogenic activity and decreased vascularization seem to be the major factors [4]. Determining how to promote osteogenesis and angiogenesis and inhibit adipogenesis in ONFH is therefore a crucial part of treatment.

It is well known that the β-catenin signaling pathway contributes to osteogenic differentiation while reducing adipogenic differentiation in the bone marrow microenvironment [5]. In addition, previous studies have suggested that the Wnt/β-catenin pathway is intimately connected to the differentiation and development of the

Zefeng Yu and Kunzheng Wang have contributed equally to this article.

✉ Lihong Fan
drfan2140@mail.xjtu.edu.cn

Kunzheng Wang
wkzh1955@mail.xjtu.edu.cn

[1] Department of Orthopedics, The Second Affiliated Hospital of Xi'an Jiaotong University, No. 157 Xiwu Road, Xi'an 710004, Shaanxi Province, People's Republic of China

microvasculature [6, 7]. β-catenin, a transcription factor, can be phosphorylated by a protein complex comprising glycogen synthase kinase-3 beta (GSK-3β), axin, and adenomatous polyposis coli. After β-catenin becomes phosphorylated, it is degraded by the proteasome. Lithium, which has been used to treat bipolar depression for years [8], can also activate the β-catenin signaling pathway by inactivating GSK-3β [9]. Galli et al. reported that the GSK-3β inhibitor lithium chloride promoted osteoblast differentiation of MC3T3 cells [10]. At the same time, Li et al. demonstrated that lithium chloride suppressed the adipogenic differentiation of adipose-derived mesenchymal stem cells by activating β-catenin signaling [11]. Accumulating evidence indicates that lithium chloride likely regulates the adipogenic/osteogenic activity of bone marrow-derived mesenchymal stem cells during steroid-related ONFH. Furthermore, Guo et al. reported that lithium promoted vascular remodeling after stroke through a GSK-3β-dependent pathway in the brain endothelium [12]. Simultaneously, Kaga et al. demonstrated that lithium promoted angiogenic effects in rat ischemic preconditioned myocardium through the GSK-3β/β-catenin pathway [13]. These findings suggest that lithium can enhance angiogenesis by activating the β-catenin pathway. However, to date, few studies have focused on the effects of lithium chloride treatment for steroid-related ONFH and its possible mechanisms.

Thus, in the current study, we examined the preventive effects of lithium chloride in a rat model of steroid-related ONFH by regulating the perturbation of adipogenesis, osteogenesis, and angiogenesis. In addition, we focused on the possible mechanisms involved in the preventive effects of lithium chloride after steroid-related treatment.

Materials and methods

Animals

Ninety male, 12-week-old Sprague–Dawley (SD) rats weighing 380–420 g were obtained from the Experimental Animal Center of Medical College, Xi'an Jiaotong University. The rats were specific-pathogen-free (SPF) animals kept in a clean, humidity-, and temperature-controlled environment with a 12 h light/dark cycle and free access to water and food. All experimental procedures abided strictly by the recommendations of the Experimental Animal Center of Medical College, Xi'an Jiaotong University, China, and the Ethics Committee of Xi'an Jiaotong University approved the care and use of animals in this experiment.

Establishment of the rat ONFH model

The SD rats were randomly distributed into three groups: Group M, ONFH model group ($n = 30$); Group L, lithium chloride group ($n = 30$); and Group C, control group ($n = 30$). The rats from Groups L and M underwent sequential drug administration to establish the ONFH model. The rats were given 4 mg/kg lipopolysaccharide (LPS, Sigma, St. Louis, MO, USA) intravenously every 24 h for 2 days. One day after the last injection of LPS, the rats were administered 60 mg/kg methylprednisolone (MPS; Pfizer, New York, USA) intramuscularly every 24 h for 3 days. For Groups L and M, rats were gavage fed either a daily dose of 200 mg/kg LiCl solution (Sigma, St. Louis, MO, USA) or saline for 14 consecutive days after the last injection of MPS; this was performed separately from the LPS and MPS administration. Rats from Group C underwent the same doses of saline injections and saline gavage feeding as Group M.

Hematological analysis

Three weeks after steroid administration, fifteen randomly chosen rats from each group underwent blood collection from the tail vein for hematological analysis. The serum concentrations of triglycerides (TGs), total cholesterol (TC), low density lipoprotein (LDL), and high density lipoprotein (HDL) were analyzed to detect the hyperlipidemia-improving effects of lithium chloride.

Micro-CT scanning

Micro-CT scanning was used to measure the micro-structure of rat femoral heads. Ten rats in each group were chosen for evaluation 28 days after the last injection of MPS. Half of the randomly selected rats underwent micro-CT angiogenesis analysis. Briefly, after the administration of phenobarbital sodium for general anesthesia, a silicone rubber injection compound (Microfil MV-122; Flow Tech, Carver, MA, USA) was perfused into the aorta ventralis, with the abdominal cavity opened, as previously reported [14]. After decalcification, these samples underwent micro-CT-based angiography. The blood vessel volume and percentage of vessel volume were quantified for angiogenesis analysis. Simultaneously, the proximal femurs of the remaining fifteen rats underwent micro-CT scanning to analyze the bone structure, as per Low et al. [15]. Bone mineral density (BMD), bone volume/total volume (BV/TV), trabecular number (Tb.N), and trabecular separation (Tb.Sp) were quantified to determine the relative amount of bone within the femoral head.

Tissue sample preparation and histology

Four weeks after the final injection of MPS, five rats from each group were sacrificed via intravenous injection of excess phenobarbital sodium. Femur samples from these rats, together with the samples that underwent micro-CT bone scanning, were promptly fixed in 10 % neutral buffered formalin for 3 days after harvesting and were decalcified with 10 % ethylene diamine tetraacetic acid for approximately 1 month. Subsequently, the decalcified femoral head samples (including the samples that underwent micro-CT-based angiography) were embedded in paraffin. Samples were then sectioned into 4-μm-thick layers and stained with hematoxylin-eosin. The ratio of empty lacunae in the bone was evaluated microscopically. During an examination of the trabeculae at ×200 magnification, 50 bone lacunae were counted in each randomly chosen field. The ratio of empty bone lacunae was also calculated.

Immunohistochemical staining

Immunohistochemistry was performed for vascular endothelial growth factor (VEGF), peroxisome proliferator-activated receptor gamma (PPARγ), and bone morphogenetic protein-2 (BMP-2). Briefly, sections from the paraffin-embedded samples were incubated for 10 min with 3 % H_2O_2. For antigen retrieval, the sections were immersed in 0.1 % trypsinase solution at 37 °C for 5–30 min. After incubation with 10 % goat antiserum (Vector, Burlingame, CA, USA) for 30 min at 25 °C, sections were treated with a primary antibody against rat PPARγ, BMP-2, or VEGF (rabbit antibodies, all from Santa Cruz Biotechnology, Inc., Dallas, Texas, USA) for 14 h at 4 °C, treated with biotin-labeled secondary antibody for 30 min, and incubated with horseradish peroxidase-conjugated streptavidin for 30 min at 25 °C. To reveal immunoreactivity, the sections were treated with diaminobenzidine solution in the dark. The sections were then treated with hematoxylin and mounted. To localize and identify areas with positively stained cells, Image-Pro Plus 6.0 was used for quantitative analysis at a magnification of ×200. For VEGF and PPARγ staining, random fields in bone marrow cavities were selected, and for BMP-2 staining, random fields in bone marrow cavities and bone trabeculae were selected. Positive staining was quantitated based on integrated optical density (IOD). The corresponding area was also measured. The results were defined as the ratio of IOD to the corresponding area.

Quantitative reverse-transcription polymerase chain reaction

Four weeks after the last injection of MPS, femoral head samples from the remaining 45 rats were quick-frozen in liquid nitrogen and ground into homogenized powder after harvesting. TRIzol reagent was used to extract the total RNA. After extraction, samples were centrifuged at 12000 rpm for 10 min at 4 °C. Then, RNA was reverse-transcribed into complementary DNA for 60 min at 42 °C, again for 15 min at 72 °C and combined with the RT-PCR mixture (Takara Bio Inc., Tokyo, Japan). The qRT-PCR assay was conducted within the mixture using SYBR Green PCR Master Mix (Roche Diagnostics, Basel, Switzerland). In our study, *β-actin* was the housekeeping gene used to standardize mRNA levels. The primers used in our study were as follows: *β-catenin*, sense 5′-GCG TCA ACA CCA TCA TTC TG-3′, antisense 5′-GCG TCA ACA CCA TCA TTC TG-3′; *GSK-3β*, sense 5′-CTG CCC TCT TCA ACT TTA CC-3′, antisense 5′-TAT TGG TCT GTCCACGGTCT-3′; and *β-actin*, sense 5′-AGT ACC CCA TTG AAC ACG GC-3′, antisense 5′-TTT TCA CGG TTA GCC TTA GG-3′. The qRT-PCR results were analyzed by SDS 2.0 (Life Technologies, Foster City, CA, USA).

Western blot

The amounts of p-Tyr^{216} GSK-3β, total GSK-3β, and β-catenin proteins in the remaining 45 rats from the three groups were detected by Western blot analysis. Total proteins (20 μg/lane) were separated by 10 % sodium dodecyl sulfate polyacrylamide gel electrophoresis and transferred onto polyvinylidene fluoride blotting membranes. The primary antibody was incubated on the membrane for 12 h at 4 °C after non-specific blocking with 5 % bovine serum albumin in Tween-Tris Buffered Saline. The following primary antibodies were used: β-catenin, p-Tyr^{216} GSK-3β and total GSK-3β antibodies (all from Santa Cruz Biotechnology, Inc., Dallas, Texas, USA) and a β-actin antibody (Boster, Wuhan, Hubei, China). Subsequently, the membranes were treated with horseradish peroxidase-labeled secondary antibody (ZDR-5306; Zhongshan Golden Bridge Biotechnology, Beijing, China) for 2 h at 37 °C. Immunoreactive proteins on the blots were visualized with ECL™ Western blotting detection reagents (GE Healthcare Life Sciences, Pittsburgh, PA, USA), and the signals were analyzed with Image Station 4000R (Kodak, Rochester, New York, USA).

Statistical analysis

The data are presented as the mean ± standard deviation (SD). A one-way analysis of variance followed by an LSD *t* test was used for comparisons among experimental groups, and Fisher's exact probability test was performed for the count data. SPSS 21.0 was used for statistical analysis. $P < 0.05$ was considered statistically significant.

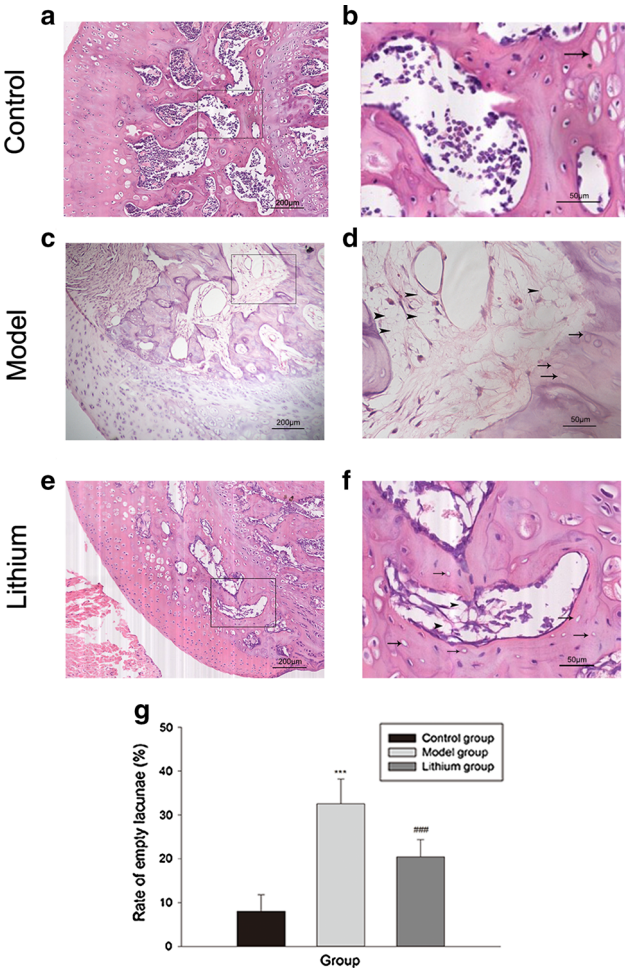

Fig. 1 Histological analysis of rat femoral heads. The model group showed many empty lacunae surrounded by necrotic marrow cells (**c**, **d**). In the lithium group, fewer empty bone lacunae and necrotic cells were observed (**e**, **f**). In the control group, no sign of ONFH was observed by microscopy (**a**, **b**). *Bar graphs* show the ratio of empty bone lacunae. The empty bone lacunae ratios in the control and lithium groups were smaller than that in the model group (**g**). Empty lacunae are indicated by *black arrows*, and necrotic adipocytes are indicated by *black arrowheads*. The *black blocks* indicate the magnified area (**a**, **c** and **e**). The data are shown as the mean ± SD. $^{***}P < 0.001$ compared with the control group. $^{\#\#\#}P < 0.001$ compared with the model group. Magnification: ×100 (**a**, **c** and **e**), ×400 (**b**, **d** and **f**)

Fig. 2 Lithium prevents blood vessel loss. The vessel structure in the model group was not clear in the femoral head regions, whereas the samples in the lithium group showed more vessels, and the samples in the control group showed an extensive vascular structure (**a**–**c**). The model group showed significantly lower blood vessel volumes and volume percentages compared with the control and lithium groups (**d**, **e**). Immunohistochemical staining of VEGF in the model group (**g**) was less intense than that in the lithium (**h**) and control groups (**f**, **i**). The data are presented as the mean ± SD. $^{***}P < 0.001$ compared with the control group. $^{\#\#\#}P < 0.001$ compared with the model group. Magnification: ×200 (**f**–**h**)

Results

Histological analysis

In this study, we defined osteonecrosis as the diffuse presence of empty lacunae or pyknotic nuclei in osteocytes in the bone trabeculae, accompanied by surrounding bone marrow cell necrosis [16]. Histological analysis indicated that osteonecrosis developed in 11 of the 15 rats in the model group and in 3 of the 15 rats in the lithium group. Fisher's exact probability test showed that the osteonecrosis incidence in the lithium group was significantly lower than that in the model group ($P < 0.01$). No rats in the control group were diagnosed with osteonecrosis. Osteonecrotic changes in the rat femoral heads were histologically examined in the three groups to assess the effects of lithium chloride on steroid-related ONFH. ONFH changes in the model group were apparent (Fig. 1c, d). Many empty lacunae were observed. The bone marrow also showed necrotic changes in hematopoietic cells and adipocytes (the loss of either nuclei or distinct cell borders of fat cells). Decreased osteonecrotic changes were observed in the lithium group, with fewer empty bone lacunae and necrotic bone marrow cells (Fig. 1e, f). In the control group, no sign of ONFH was observed by microscopy (Fig. 1a, b). The rate of empty lacunae in the model group was significantly higher than that in the lithium and control groups ($P < 0.001$, $n = 15$, Fig. 1g).

Lithium prevents blood vessel loss in steroid-related ONFH in rats

The micro-structures of blood vessels from the three groups were rebuilt three-dimensionally. The vessel structure in the model group was not clear in and around the femoral head, whereas the samples in the lithium group had significantly more microvessels, and the specimens in the control group had extensive vascular microstructures (Fig. 2a–c). Quantitatively, the model group had significantly lower blood vessel volumes and volume percentages compared with the lithium and control groups ($P < 0.001$,

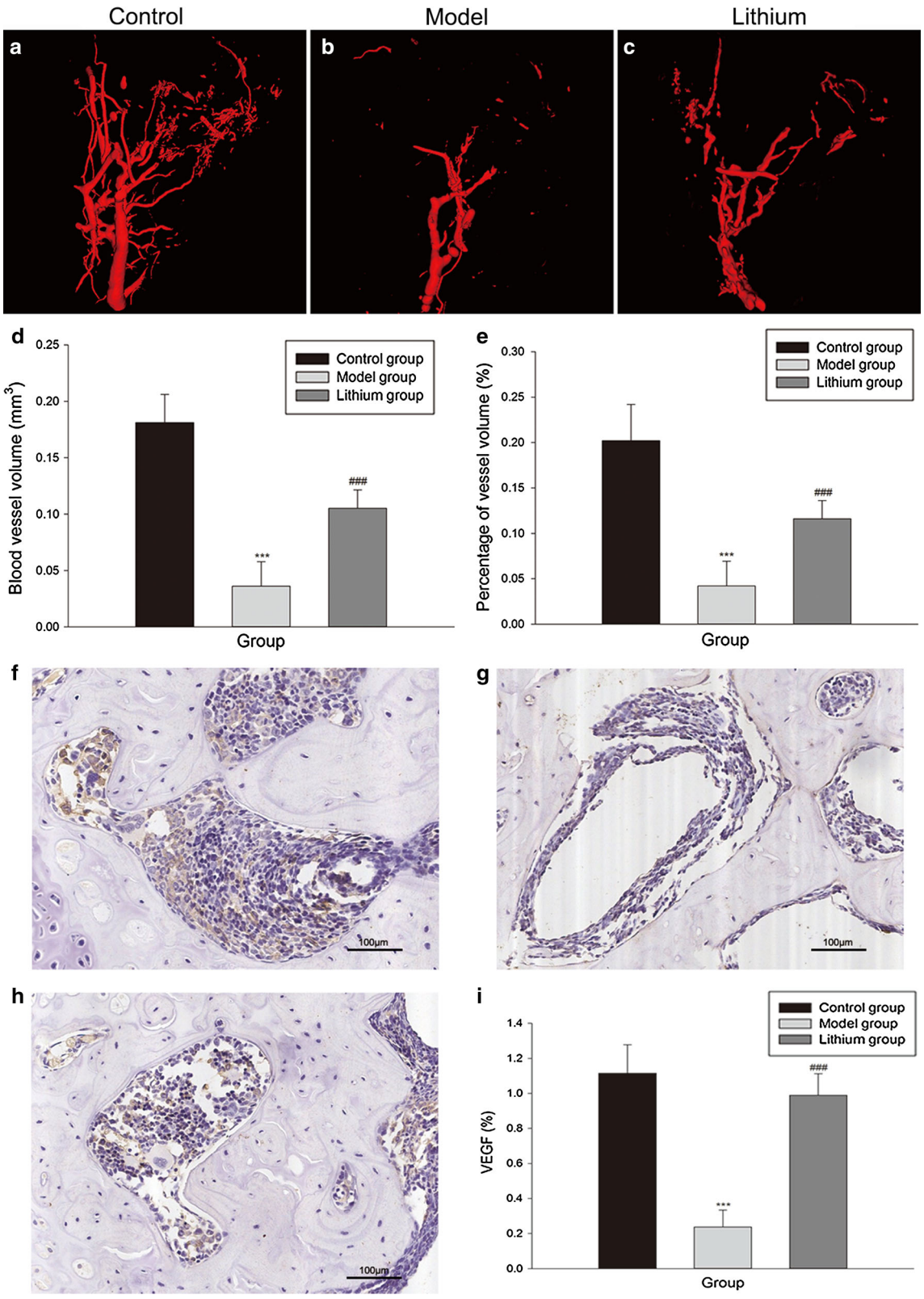
Control
Model
Lithium
a
b
c
d
Blood vessel volume (mm3)
0.25
0.20
0.15
0.10
0.05
0.00
Control group
Model group
Lithium group
***
###
Group
e
Percentage of vessel volume (%)
0.30
0.25
0.20
0.15
0.10
0.05
0.00
Control group
Model group
Lithium group
***
###
Group
f
100μm
g
100μm
h
100μm
i
VEGF (%)
1.4
1.2
1.0
0.8
0.6
0.4
0.2
0.0
Control group
Model group
Lithium group
***
###
Group

$n = 10$, Fig. 2d, e). In addition, immunohistochemical staining for VEGF, which usually indicates potential angiogenic function (Fig. 2g), was significantly lower in the model group than in the control (Fig. 2f) and lithium groups (Fig. 2h) ($P < 0.001$, $n = 15$, Fig. 2i).

Lithium reduces serum lipids and adipogenesis in steroid-related ONFH in rats

We also performed serum lipid tests. The lithium and model groups had significantly higher concentrations of serum TGs, TC, and LDL and significantly lower levels of HDL compared with the control group. Compared with the model group, the lithium group had a significantly improved hyperlipidemic state (lower serum TGs, TC, and LDL and higher HDL; $P < 0.001$, $n = 15$, Fig. 3a–d). We also performed immunohistochemical staining of PPARγ to evaluate adipogenesis in the femoral heads. As shown in Fig. 3f, PPARγ was observed in the rat femoral heads from the model group with highly positive immunoreactivity. Significantly stronger PPARγ immunoreactivity was found in the steroid-related ONFH group than in the lithium (Fig. 3g) and control groups (Fig. 3e) ($P < 0.001$, $n = 15$, Fig. 3h).

Lithium prevents bone loss in steroid-related ONFH in rats

We used micro-CT bone scanning to analyze the bone structure in the rat femoral heads. The micro-CTs showed that the subchondral bone in the rat femoral heads was finely spread and holonomic in the control group (Fig. 4a). In the ONFH model group, the subchondral trabeculae were damaged (Fig. 4b). The results of the lithium group were intermediate compared with the other two groups ($n = 10$, Fig. 4c). The comprehensive quantitative analysis of all micro-CT parameters confirmed that the microstructure of the subchondral trabeculae in the femoral heads from the model group was weaker than that in the control and lithium groups ($n = 10$, Fig. 4d–g). In addition, the immunohistochemical staining of BMP-2, which usually suggests potential osteogenic function, was significantly less in the model group (Fig. 4i) than those in the control (Fig. 4h) and lithium groups (Fig. 4j) ($P < 0.001$, $n = 15$, Fig. 4k).

Lithium counteracts the negative effects of steroids on GSK-3β and β-catenin protein abundance in steroid-related ONFH in rats

Total GSK-3β, p-Tyr^{216} GSK-3β and β-catenin protein levels, and GSK-3β and β-catenin mRNA expression levels were assessed in femoral heads. Figure 5a shows that steroid-related treatment significantly increased GSK-3β mRNA expression and decreased β-catenin mRNA expression compared with the control group ($P < 0.001$, $n = 15$). Moreover, lithium treatment could reverse these changes. At the protein level, increased p-Tyr^{216} GSK-3β and decreased β-catenin were observed in the model group compared with the control group ($P < 0.001$, $n = 15$, Fig. 5b, c). Furthermore, Western blot analysis showed that lithium treatment significantly upregulated β-catenin protein expression and decreased p-Tyr^{216} GSK-3β ($P < 0.001$, $n = 15$, Fig. 5b, c). Meanwhile, total GSK-3β protein levels did not show a statistically significant difference among the three groups ($P > 0.05$, $n = 15$, Fig. 5b, c).

Fig. 3 Lithium reduces serum lipids and adipogenesis. The lithium and model groups had significantly higher levels of serum TC, TGs, and LDL and significantly lower levels of HDL compared with the control and lithium groups (**a–d**). PPARγ was observed in the rat femoral heads from the model group, with highly positive immunoreactivity (**f**). Significantly stronger PPARγ immunoreactivity was found in the steroid-related ONFH group than in the lithium (**g**) and control groups (**e**, **h**). The data are presented as the mean ± SD. $^{***}P < 0.001$ compared with the control group. $^{\#\#\#}P < 0.001$ compared with the model group. Magnification: ×200 (**e–g**)

Discussion

Steroid-related ONFH is a frequently occurring disease that can lead to necrosis of bone tissue and arthritis of the hip joint. However, the exact pathogenesis of this disease remains unknown. Interruption of the microcirculation of the femoral head is considered by the final pathway leading to steroid-related ONFH [17, 18]. In addition, several studies have demonstrated that excess steroid usage can damage the equilibrium between osteogenesis and adipogenesis in the femoral head [19, 20]. Lithium, a known GSK-3β inhibitor, was recently reported to reduce adipocyte differentiation and improve angiogenesis and osteogenesis [12, 21, 22]. Additionally, GSK-3β activity is regulated by phosphorylation, and Tyr216 phosphorylation increases its activity [23]. Garza et al. have demonstrated that steroids inhibit β-catenin signaling by activating GSK-3β with increasing levels of p-Tyr^{216} GSK-3β protein [24]. Thus, in this study, we explored whether lithium could prevent steroid-related ONFH in rats by reversing the perturbation of osteogenic/adipogenic activity and promoting angiogenesis via β-catenin activation.

Based on a study by Okazaki et al. [25], we generated a modified rat steroid-related ONFH model in which the LPS dosage was doubled and the dosage of MPS was tripled. As a result, the frequency of osteonecrosis was much higher in our study. We found that the ONFH model showed the histopathological characteristics of empty lacunae and

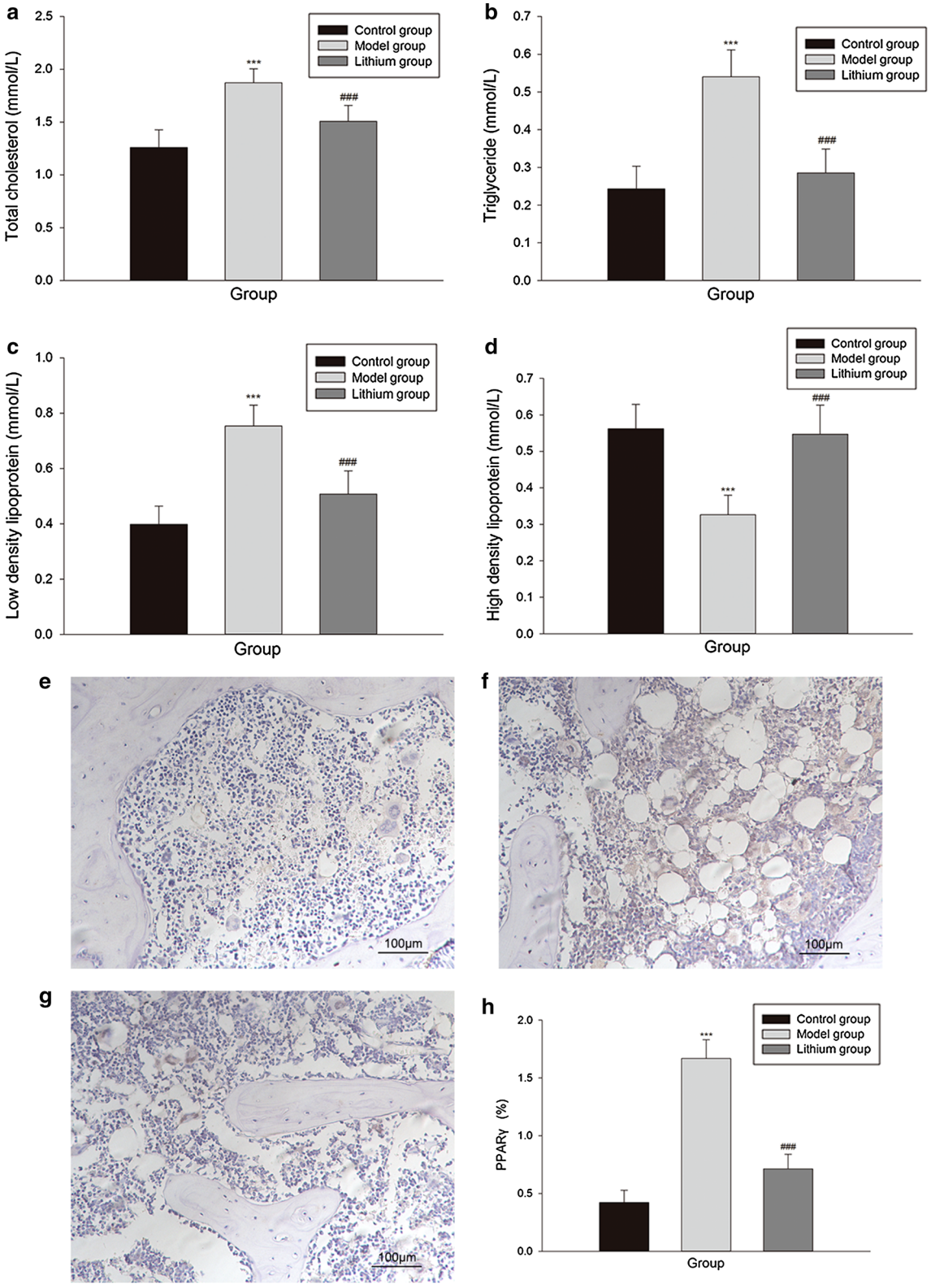
a
Total cholesterol (mmol/L)
2.5
2.0
1.5
1.0
0.5
0.0
***
###
Control group
Model group
Lithium group
Group
b
Triglyceride (mmol/L)
0.7
0.6
0.5
0.4
0.3
0.2
0.1
0.0
***
###
Control group
Model group
Lithium group
Group
c
Low density lipoprotein (mmol/L)
1.0
0.8
0.6
0.4
0.2
0.0
***
###
Control group
Model group
Lithium group
Group
d
High density lipoprotein (mmol/L)
0.7
0.6
0.5
0.4
0.3
0.2
0.1
0.0
***
###
Control group
Model group
Lithium group
Group
e
100μm
f
100μm
g
100μm
h
PPARγ (%)
2.0
1.5
1.0
0.5
0.0
***
###
Control group
Model group
Lithium group
Group

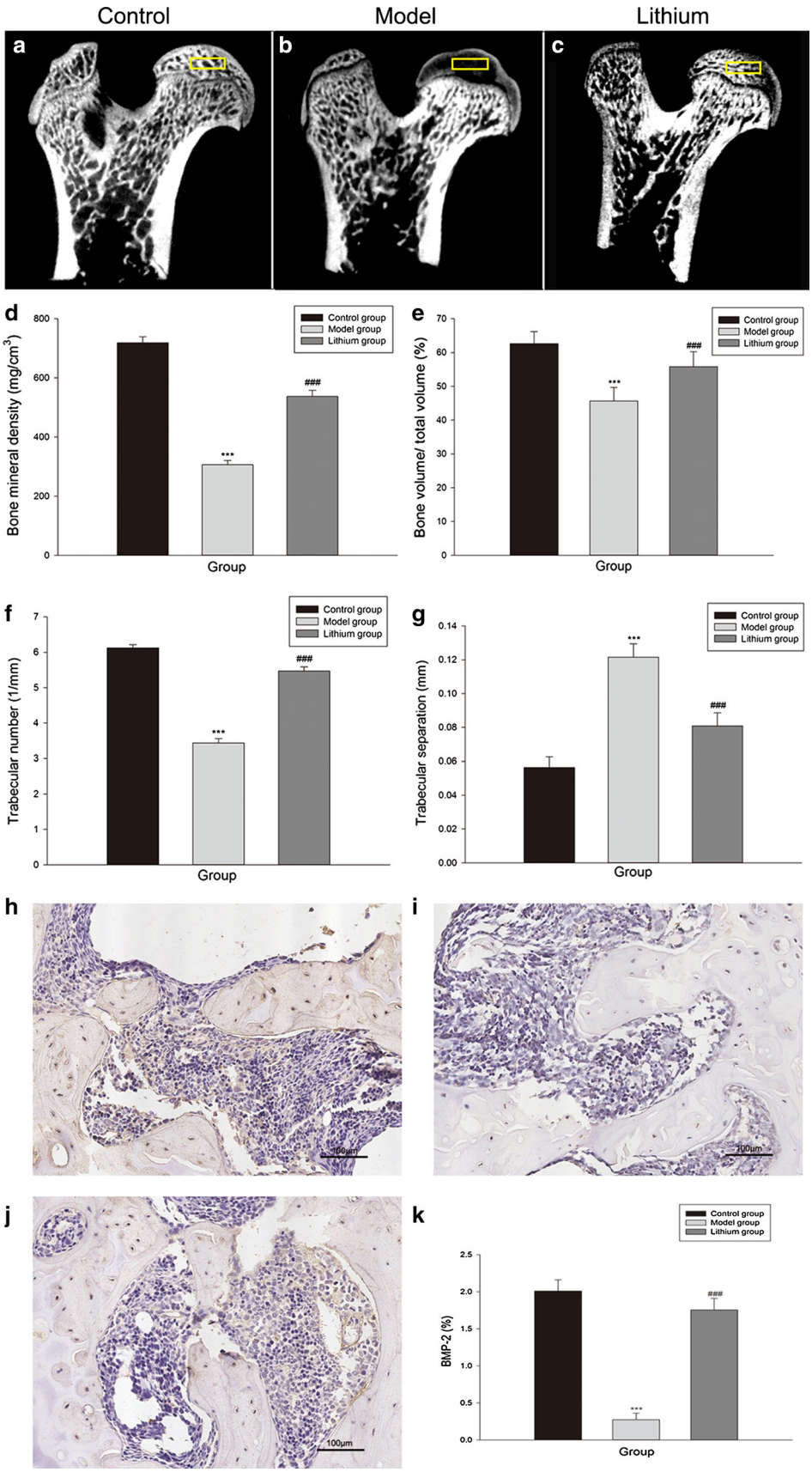

Fig. 4 Lithium prevents bone loss. The *yellow blocks* (three-dimensional spaces present in two-dimensional areas) indicate the region of interest (ROI, 1.5 mm × 1.5 mm × 0.5 mm) in the rat femoral heads of the three groups (**a**–**c**). The ROI in the model group shows that the subchondral trabeculae were damaged (**b**). The ROI in the lithium group shows an improved distribution of subchondral trabeculae (**c**). The ROI in the control group shows the most optimal structure among the three groups (**a**). BMD, BV/TV, and Tb.N in the ONFH model group were significantly smaller than in the other two groups (**d**–**f**). The Tb.Sp was significantly larger in the model group than in the other groups (**g**). Immunohistochemical staining of BMP-2 in the model group (**i**) was less than in the control (**h**) and lithium groups (**j**, **k**). The data are presented as the mean ± SD. $^{***}P < 0.001$ compared with the control group. $^{###}P < 0.001$ compared with the model group. Magnification: ×200 (**h**–**j**)

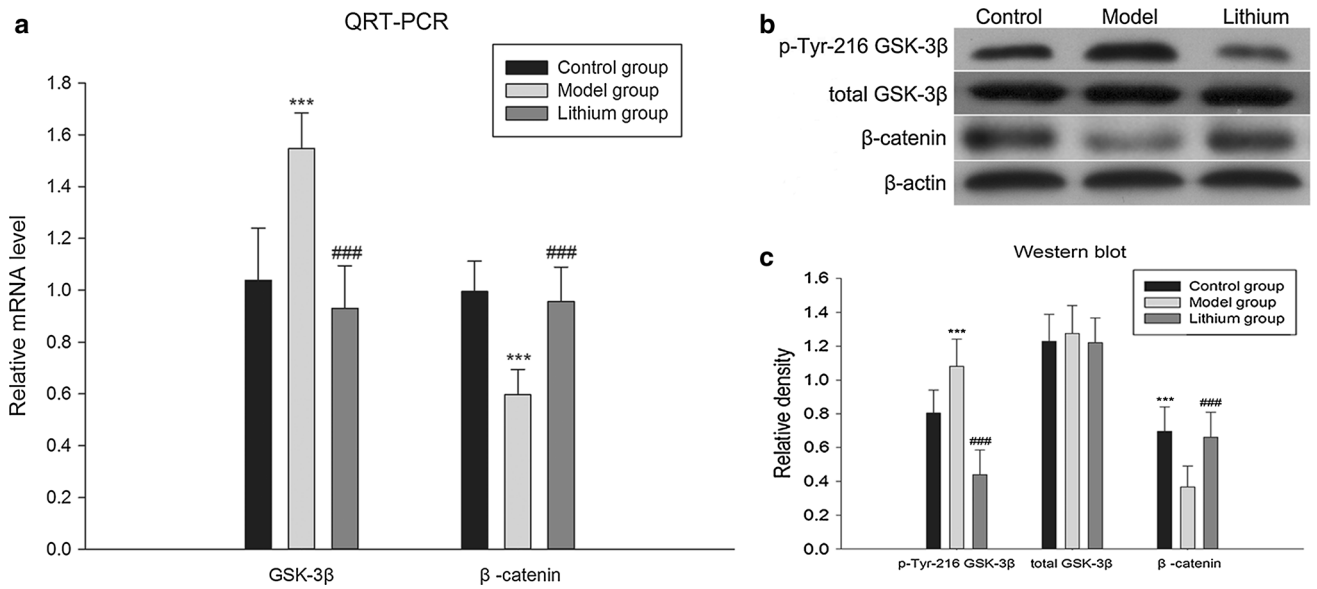

Fig. 5 Lithium promotes β-catenin abundance. The model group showed significantly decreased β-catenin and increased GSK-3β mRNA levels compared with the lithium and control groups (**a**). Increased p-Tyr^{216} GSK-3β and decreased β-catenin protein levels were observed in the model group compared with the other groups (**b**, **c**). Total GSK-3β protein levels among three groups did not show any statistically significant difference (**b**, **c**). The data are presented as the mean ± SD. $^{***}P < 0.001$ compared with the control group. $^{\#\#\#}P < 0.001$ compared with the model group

bone marrow cell necrosis. After lithium administration, the rate of empty lacunae was significantly decreased. These results indicate that lithium can prevent steroid-related ONFH. We also found decreased β-catenin and increased p-Tyr^{216} GSK-3β (the active form of GSK-3β) levels after steroid-related treatment, which was consistent with the results of Garza et al. [24].

In our study, we chose micro-CT-based microangiography to analyze the blood circulation of the femoral head. We found significantly more blood vessels in the lithium and normal groups compared with the model group. This result suggests that lithium may improve angiopoiesis of rat femoral heads after steroid-related treatment, which is in line with previous studies showing the effects of lithium, including the improvement of vascular remodeling [12] and the promotion of angiogenic effects [13]. Lithium can increase β-catenin concentrations and activate the β-catenin pathway [10]. In the present study, we showed that lithium reduced p-Tyr^{216} GSK-3β and promoted β-catenin expression. Moreover, Zhang et al. suggested that the β-catenin pathway promotes VEGF expression [26]. Later, Easwaran et al. and Thirunavukkarasu et al. identified VEGF as a target gene of β-catenin signaling during angiogenesis [27, 28]. We showed that VEGF had significantly higher expression in the lithium treatment group than in the model group, which could be a consequence of β-catenin activation. These results indicate that lithium may enhance angiogenesis in rat femoral heads after steroid treatment by activating the β-catenin pathway.

Steroids may decrease osteogenesis and increase adipogenesis of the bone marrow during the process of ONFH [29]. Therefore, it is reasonable to infer that a method of ONFH prevention would be to attenuate disturbances in osteogenesis and adipogenesis. Indeed, PPARγ can stimulate adipogenesis in bone marrow cells and inhibit osteogenesis [30]. We found that PPARγ expression in the lithium treatment group was significantly lower than that in the model group. In addition, lithium also acted as a lipid-decreasing drug, reducing serum lipids. However, we found that the staining intensity of BMP-2, which plays a crucial role during bone formation [31], in the lithium treatment group was stronger than that in the model group. Micro-CT bone scanning also showed a significantly firmer bone structure in the lithium treatment group than in the model group. Furthermore, lithium was found to increase β-catenin expression in our study. As a result, the β-catenin pathway might be activated. Moreover, increased β-catenin expression inhibits PPARγ and suppresses adipocytic differentiation [32, 33], whereas inactivation of the β-catenin pathway increases adipogenesis [34] and reduces osteogenesis [35]. Therefore, we suggest that lithium may reduce abnormal adipogenesis and increase bone formation in steroid-related ONFH by activating the β-catenin pathway.

In conclusion, our data indicate that the local β-catenin pathway is inhibited during steroid-related ONFH. Our study also offers evidence that lithium may enhance angiogenesis and stabilize osteogenic/adipogenic homeostasis in steroid-related ONFH in rats by activating the

β-catenin signaling pathway. These findings highlight that lithium administration has potential as an effective and novel therapeutic means for preventing steroid-related ONFH.

Acknowledgments This work was supported by the National Natural Science Foundation of China (Nos. 81101363, 81371944 and 81572145) and the Fundamental Research Funds for the Central Universities.

Compliance with ethical standards

Conflict of interest The authors declare that there is no conflict of interest.

References

1. J. Gagala, M. Buraczynska, T. Mazurkiewicz, A. Ksiazek, Endothelial nitric oxide synthase gene intron 4 polymorphism in non-traumatic osteonecrosis of the femoral head. Int. Orthop. **37**(7), 1381–1385 (2013). doi:10.1007/s00264-013-1892-7
2. Y.J. Lee, J.S. Lee, E.H. Kang, Y.K. Lee, S.Y. Kim, Y.W. Song, K.H. Koo, Vascular endothelial growth factor polymorphisms in patients with steroid-induced femoral head osteonecrosis. J. Orthop. Res. **30**(1), 21–27 (2012). doi:10.1002/jor.21492
3. R.S. Weinstein, Glucocorticoid-induced osteonecrosis. Endocrine **41**(2), 183–190 (2012). doi:10.1007/s12020-011-9580-0
4. J.S. Lee, L.S. Lee, H.L. Rob, C.H. Kim, J.S. Jung, K.T. Suh, Alterations in the differentiation ability of mesenchymal stem cells in patients with nontraumatic osteonecrosis of the femoral head: comparative analysis according to the risk factor. J. Orthop. Res. **24**(4), 604–609 (2006). doi:10.1002/jor.20078
5. M.E. Nuttall, J.M. Gimble, Controlling the balance between osteoblastogenesis and adipogenesis and the consequent therapeutic implications. Curr. Opin. Pharmacol. **4**(3), 199–201 (2004)
6. E. Dejana, The role of wnt signaling in physiological and pathological angiogenesis. Circ. Res. **107**(8), 943–952 (2010). doi:10.1161/circresaha.110.223750
7. E. Lammert, Developmental biology brain Wnts for blood vessels. Science **322**(5905), 1195–1196 (2008). doi:10.1126/science.1167451
8. W. Young, Review of lithium effects on brain and blood. Cell Transplant. **18**(9), 951–975 (2009). doi:10.3727/096368909x471251
9. C.M. Hedgepeth, L.J. Conrad, J. Zhang, H.C. Huang, V.M.Y. Lee, P.S. Klein, Activation of the wnt signaling pathway: a molecular mechanism for lithium action. Dev. Biol. **185**(1), 82–91 (1997). doi:10.1006/dbio.1997.8552
10. C. Galli, M. Piemontese, S. Lumetti, E. Manfredi, G.M. Macaluso, G. Passeri, GSK3b-inhibitor lithium chloride enhances activation of Wnt canonical signaling and osteoblast differentiation on hydrophilic titanium surfaces. Clin. Oral Implant Res. **24**(8), 921–927 (2013). doi:10.1111/j.1600-0501.2012.02488.x
11. H.-X. Li, X. Luo, R.-X. Liu, Y.-J. Yang, G.-S. Yang, Roles of Wnt/beta-catenin signaling in adipogenic differentiation potential of adipose-derived mesenchymal stem cells. Mol. Cell. Endocrinol. **291**(1–2), 116–124 (2008). doi:10.1016/j.mce.2008.05.005
12. S. Guo, K. Arai, M.F. Stins, D.-M. Chuang, E.H. Lo, Lithium upregulates vascular endothelial growth factor in brain endothelial cells and astrocytes. Stroke **40**(2), 652–655 (2009). doi:10.1161/strokeaha.108.524504
13. S. Kaga, L.J. Zhan, E. Altaf, N. Maulik, Glycogen synthase kinase-3 beta/beta-catenin promotes angiogenic and anti-apoptotic signaling through the induction of VEGF, Bcl-2 and survivin expression in rat ischemic preconditioned myocardium. J. Mol. Cell. Cardiol. **40**(1), 138–147 (2006). doi:10.1016/j.yjmcc.200509.009
14. Y. Sun, Y. Feng, C. Zhang, The effect of bone marrow mononuclear cells on vascularization and bone regeneration in steroid-induced osteonecrosis of the femoral head. Joint Bone Spine **76**(6), 685–690 (2009). doi:10.1016/j.jbspin.2009.04.002
15. S.C. Low, G.I. Bain, D.M. Findlay, K. Eng, E. Perilli, External and internal bone micro-architecture in normal and Kienbock's lunates: a whole-bone micro-computed tomography study. J. Orthop. Res. **32**(6), 826–833 (2014). doi:10.1002/jor.22611
16. T. Yamamoto, T. Irisa, Y. Sugioka, K. Sueishi, Effects of pulse methylprednisolone on bone and marrow tissues—corticosteroid-induced osteonecrosis in rabbits. Arthritis Rheum. **40**(11), 2055–2064 (1997). doi:10.1002/art.1780401119
17. C. Powell, C. Chang, M.E. Gershwin, Current concepts on the pathogenesis and natural history of steroid-induced osteonecrosis. Clin. Rev. Allergy Immunol. **41**(1), 102–113 (2011). doi:10.1007/s12016-010-8217-z
18. H.S. Kim, S.C. Bae, T.H. Kim, S.Y. Kim, Endothelial nitric oxide synthase gene polymorphisms and the risk of osteonecrosis of the femoral head in systemic lupus erythematosus. Int. Orthop. **37**(11), 2289–2296 (2013). doi:10.1007/s00264-013-1966-6
19. R. Takano-Murakami, K. Tokunaga, N. Kondo, T. Ito, H. Kitahara, M. Ito, N. Endo, Glucocorticoid inhibits bone regeneration after osteonecrosis of the femoral head in aged female rats. Tohoku J. Exp. Med. **217**(1), 51–58 (2009)
20. L. Yin, Y.B. Li, Y.S. Wang, Dexamethasone-induced adipogenesis in primary marrow stromal cell cultures: mechanism of steroid-induced osteonecrosis. Chin. Med. J. **119**(7), 581–588 (2006)
21. S. Lee, W.K. Yang, J.H. Song, Y.M. Ra, J.-H. Jeong, W. Choe, I. Kang, S.-S. Kim, J. Ha, Anti-obesity effects of 3-hydroxychromone derivative, a novel small-molecule inhibitor of glycogen synthase kinase-3. Biochem. Pharmacol. **85**(7), 965–976 (2013). doi:10.1016/j.bcp.2012.12.023
22. N.K. Satija, D. Sharma, F. Afrin, R.P. Tripathi, G. Gangenahalli, High throughput transcriptome profiling of lithium stimulated human mesenchymal stem cells reveals priming towards osteoblastic lineage. Plos One **8**(1), e55769 (2013). doi:10.1371/journal.pone.0055769
23. K. Hughes, E. Nikolakaki, S.E. Plyte, N.F. Totty, J.R. Woodgett, Modulation of the glycogen synthase kinase-3 family by tyrosine phosphorylation. EMBO J. **12**(2), 803–808 (1993)
24. J.C. Garza, M. Guo, W. Zhang, X.Y. Lu, Leptin restores adult hippocampal neurogenesis in a chronic unpredictable stress model of depression and reverses glucocorticoid-induced inhibition of GSK-3 beta/beta-catenin signaling. Mol. Psychiatry **17**(8), 790–808 (2012). doi:10.1038/mp.2011.161
25. S. Okazaki, Y. Nishitani, S. Nagoya, M. Kaya, T. Yamashita, H. Matsumoto, Femoral head osteonecrosis can be caused by disruption of the systemic immune response via the toll-like receptor 4 signalling pathway. Rheumatology **48**(3), 227–232 (2009). doi:10.1093/rheumatology/ken462
26. X.B. Zhang, J.P. Gaspard, D.C. Chung, Regulation of vascular endothelial growth factor by the Wnt and K-ras pathways in colonic neoplasia. Cancer Res. **61**(16), 6050–6054 (2001)
27. V. Easwaran, S.H. Lee, L. Inge, L. Guo, C. Goldbeck, E. Garrett, M. Wiesmann, P.A. Garcia, J.H. Fuller, V. Chan, F. Randazzo, R. Gundel, R.S. Warren, J. Escobedo, S.L. Aukerman, R.N. Taylor, W.J. Fantl, Beta-catenin regulates vascular endothelial growth factor expression in colon cancer. Cancer Res. **63**(12), 3145–3153 (2003)

28. M. Thirunavukkarasu, Z. Han, L. Zhan, S.V. Penumathsa, V.P. Menon, N. Maulik, Adeno-sh-beta-catenin abolishes ischemic preconditioning-mediated cardioprotection by downregulation of its target genes VEGF, Bcl-2, and survivin in ischemic rat myocardium. Antioxid. Redox Signal. **10**(8), 1475–1484 (2008). doi:10.1089/ars.2008.2042
29. T.-H. Kim, J.M. Hong, F.K. Park, S.-Y. Kim, Peroxosome proliferator-activated receptor-gamma gene polymorphisms are not associated with ostenecrosis of the femoral head on the Korean population. Mol. Cells **24**(3), 388–393 (2007)
30. J. Watt, J.J. Schlezinger, Structurally-diverse, PPARgamma-activating environmental toxicants induce adipogenesis and suppress osteogenesis in bone marrow mesenchymal stromal cells. Toxicology **331**, 66–77 (2015). doi:10.1016/j.tox.2015.03.006
31. T.K. Sampath, J.E. Coughlin, R.M. Whetstone, D. Banach, C. Corbett, R.J. Ridge, E. Ozkaynak, H. Oppermann, D.C. Rueger, Bovine osteogenic protein is composed of dimers of OP-1 and BMP-2A, 2 members of the transforming growth-factor-beta superfamily. J. Biol. Chem. **265**(22), 13198–13205 (1990)
32. S.E. Ross, N. Hemati, K.A. Longo, C.N. Bennett, P.C. Lucas, R.L. Erickson, O.A. MacDougald, Inhibition of adipogenesis by Wnt signaling. Science **289**(5481), 950–953 (2000). doi:10.1126/science.289.5481.950
33. J.J. Liu, S.R. Farmer, Regulating the balance between peroxisome proliferator-activated receptor gamma and beta-catenin signaling during adipogenesis—a glycogen synthase kinase 3 beta phosphorylation-defective mutant of beta-catenin inhibits expression of a subset of adipogenic genes. J. Biol. Chem. **279**(43), 45020–45027 (2004). doi:10.1074/jbc.M407050200
34. C.N. Bennett, S.E. Ross, K.A. Longo, L. Bajnok, N. Hemati, K.W. Johnson, S.D. Harrison, O.A. MacDougald, Regulation of Wnt signaling during adipogenesis. J. Biol. Chem. **277**(34), 30998–31004 (2002). doi:10.1074/jbc.M204527200
35. E.E. Beier, T.J. Sheu, T. Buckley, K. Yukata, R. O'Keefe, M.J. Zuscik, J.E. Puzas, Inhibition of beta-catenin signaling by Pb leads to incomplete fracture healing. J. Orthop. Res. **32**(11), 1397–1405 (2014). doi:10.1002/jor.22677